Journal of Process Control 24 (2014) 1609–1626

Contents lists available at ScienceDirect

Journal of Process Control

journal homepage: www.elsevier.com/locate/jprocont

Fuzzy modeling and stable model predictive tracking control of large-scale power plants

Xiao Wu [a,*], Jiong Shen [a], Yiguo Li [a], Kwang Y. Lee [b]

[a] Department of Energy Information and Automation, Southeast University, Nanjing 210096, China
[b] Department of Electrical and Computer Engineering, Baylor University, One Bear Place #97356, Waco, TX 76798-7356, USA

ARTICLE INFO

Article history:
Received 21 November 2013
Received in revised form 17 June 2014
Accepted 6 August 2014
Available online 2 September 2014

Keywords:
Power plant
Stable model predictive control
Subspace identification
Fuzzy clustering
TS-fuzzy model

ABSTRACT

This paper develops a stable model predictive tracking controller (SMPTC) for coordinated control of a large-scale power plant. First, a Takagi–Sugeno (TS) fuzzy model is established to approximate the behavior of the boiler–turbine coordinated control system (CCS) using fuzzy clustering and subspace identification (SID). Then, an SMPTC is designed based on the fuzzy model to track the power and pressure set-points while guaranteeing the input-to-state stability and the input constraints of the system. An output-based objective function is adopted for the proposed SMPTC so that the controller could be directly applicable for the data-driven model. Moreover, the effect of modeling mismatches and unknown plant variations has been overcome by the use of a disturbance term and steady-state target calculator (SSTC). Simulation results for a 600 MW power plant show that an off-set free tracking performance can be achieved over a wide range load variation.

1. Introduction

Thermal power plant is the most widely used facility for power generation, which is composed by the boiler, turbine and generator to transform the fuel chemical energy into electric energy.

For a thermal power plant, the main task of the control system is to regulate the power output to meet the demand of the grid while maintaining the throttle pressure within a given tolerance to keep the power plant in a safe operating condition. Such an object is generally achieved by the multi-loop proportional–integral–derivative (PID) controllers, under either the boiler-following or turbine-following control mode [1]. However, in the context of increasing power demand as well as the energy and environmental issues, power plants are increasing in size and becoming more complex in order to achieve high efficiency and the scale of economy. Therefore, power plants present a challenging control problem owing to the behaviors such as: severe nonlinearity over a wide operation range, tight operating constraints, strong coupling among the multitude of variables, unknown disturbances and plant parameter variations. Consequently, the conventional PI/PID based controllers are no longer sufficient in meeting performance specifications, even if they are well tuned at a given load level; thus, various control strategies have been extensively studied [1–20].

As a direct approach to improve the conventional PI/PID controller, auto-tuning of the PID parameters is studied in [1–4] utilizing the fuzzy logic, particle swarm optimization (PSO) and iterative feedback tuning (IFT). In [5], a single linear controller is designed on the basis of careful choice of the operating range to avoid severe nonlinearity. In [6], a gain-scheduled l^1-optimal approach is designed for the boiler–turbine unit based on the linear parameter varying model. In [7,8], H_∞ controllers are proposed to enhance the robustness of power plant control system. To overcome the nonlinearity of the power plant, various artificial intelligence techniques have also been applied. In [9], a fuzzy auto-regressive moving average (FARMA) controller was applied to the boiler–turbine system with rules generated using the history of input–output data. In [10], a linear quadratic regulator (LQR) controller is designed for the boiler–turbine through the genetic algorithm.

However, none of these controllers except [6] have dealt with the input constraints in the controller design stage; therefore, model predictive controller (MPC) has been employed in recent years. In [11], a dynamic matrix control (DMC) is employed for the boiler–turbine.

* Corresponding author. Tel.: +86 13645166145; fax: +86 25 83795951.
E-mail addresses: wux@seu.edu.cn (X. Wu), shenj@seu.edu.cn (J. Shen), lyg@seu.edu.cn (Y. Li), Kwang_Y_Lee@baylor.edu (K.Y. Lee).

http://dx.doi.org/10.1016/j.jprocont.2014.08.007
0959-1524/

It shows that the step-response model based on the test data is better suited than using the linearized mathematical model, but the performance of the proposed linear controller is degraded in a wide range operation. In [12,13] nonlinear predictive controllers are designed based on the neural network model and input–output feedback linearization. Although the control performance is improved, the nonlinear optimization is time consuming and lacks robustness.

To overcome these issues, the fuzzy modeling technique [21], which uses a combination of several linear models to approximate the nonlinear behavior of the plant, has been widely used in controller design for a wide range power plant operation [14–19], resulting in better performance than the conventional MPC methods. In [14–18], various kinds of MPCs are proposed on the Takagi–Sugeno (TS) fuzzy model for the boiler–turbine coordinated system, utilizing different computational algorithms, such as linear matrix inequalities (LMIs) [14], genetic algorithm (GA) [15,17], quadratic programming (QP) [16], and iterative learning [18]. In [19], a generalized predictive controller (GPC) is designed on the basis of neuro-fuzzy network model to control the steam temperature system of a 200 MW power plant. However, the stability of the control system which is desirable for industrial processes such as thermal power plant cannot be guaranteed by all of the aforementioned approaches, except [14,15].

On the other hand, it is common that, state-space models are used as local models in these fuzzy controllers [8,14–17] because of the advances in multi-variable systems and control theory for linear systems. In these works, an approximation or transformation of the nonlinear system has been used to obtain the linear state-space models. However, for complex systems such as large-scale power plant, it is difficult to develop an accurate analytical model without the knowledge of thermodynamics and design specifications of many components, and this has become one of the main limitations in designing controllers for real power plants. Moreover, except [15] the structure of the fuzzy model is designed by simply dividing the operation range evenly, which greatly affects the accuracy of the model.

For these reasons, we propose a stable model predictive tracking controller (SMPTC) based on the data-driven fuzzy model to solve power plant control problems. Firstly, a TS fuzzy model is developed to approximate the behavior of the coordinated control system (CCS) in the power plant. Compared with the ordinary methods which linearize the nonlinear mathematical model around different operating points [8,14–18], we propose the use of fuzzy clustering [22] and subspace method [23–25] to identify the local state-space model directly from input–output data. To overcome the nonlinearity of the power plant, fuzzy clustering is first used to develop the structure of the fuzzy system and the membership functions, and then by combining the data with the membership functions, the SID is extended to develop all local state-space models.

The SMPTC is then designed on the developed fuzzy model to achieve a satisfactory power output and throttle pressure performance, while satisfying the input constraints and guaranteeing the closed-loop system stability. To improve the output tracking performance of the conventional stable MPC, an output-based objective function is used in the SMPTC formulation. Offset-free control is also achieved, even in the case of modeling mismatches and unknown plant behavior variations, by introducing a disturbance term and steady-state target calculator (SSTC) [26,27]. It is shown that the SMPTC can be realized by solving a set of linear matrix inequalities (LMIs), which is known to be a computationally efficient algorithm [14,28–30].

The proposed modeling and control approaches are applied to the CCS in a 600 MW large-scale power plant simulator. The remainder of this paper is organized as follows: Section 2 describes the power plant. Section 3 establishes the TS-fuzzy model of the CCS using fuzzy clustering and subspace identification. The SMPTC is developed in Section 4, and simulation results are given in Section 5. Finally, some conclusions are drawn in Section 6.

2. System description

The power plant under consideration is a 600 MW oil-fired drum-type boiler–turbine–generator unit shown in Fig. 1. The model of this plant is developed from the first-principles as used in a power plant simulator and is validated in the MATLAB environment. The model is grouped into boiler, turbine, feedwater, and condenser modules and composed of 31 subsystems and 12 control valves associated with physical processes as shown in Fig. 1 [3].

As two of the most critical variables in a power plant, the power output E and throttle pressure P are controlled by the CCS through manipulating primarily the fuel flow valve u_1 and turbine governor valve u_8. However, the variables are strongly coupled and the fuel flow has a relatively large thermal inertia property to the power and pressure. Moreover, the frequent unit load demand change brings severe nonlinearity to the CCS, and furthermore, the equipment wear, environmental change, fuel variation, etc., will result in significant disturbances and plant behavior variations. Therefore, advanced control techniques are needed to overcome the weaknesses of the conventional controllers.

3. Data-driven fuzzy modeling of the boiler–turbine coordinated control system

Subspace identification (SID) method provides an effective way to develop the state-space model directly from the input–output data of the plant [23,24]. Based on computational tools such as QR-factorization and singular value decomposition (SVD), the SID extracts the model from subspaces of data Hankel matrices. Comparing with the conventional identification methods, the SID has several distinct advantages, such as: (1) computationally efficient, especially for multivariable systems; (2) avoid local minima and convergence problems; (3) no requirement for initial conditions; and (4) the system order can be easily chosen.

However, the SID is only for linear system identification, while the power plant has inherent nonlinearity due to the load variations [12–20]. In [20], the whole operating region of the plant is first divided by using a nonlinear analysis tool (Vinnicombe gap metric, to be specific [31]), and the corresponding data for each region are collected to identify the local models separately. Then, switching point information is utilized to transform all local models into a common basis to form an integrated multi-model system. Although the resulting model can approximate the plant behavior closely, the modeling procedure is complex and greatly relying on human knowledge and intervention. As an alternative to the approach in [20], the fuzzy modeling strategy is adopted in this paper to solve the nonlinear problem by combining the fuzzy clustering with the SID.

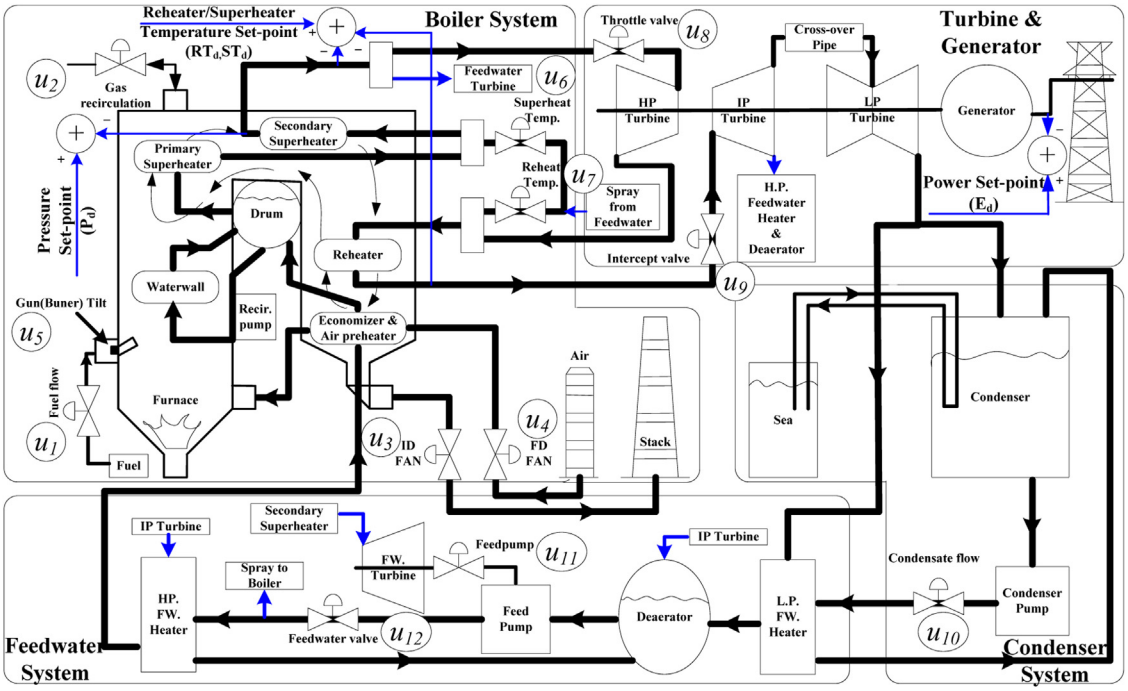

Fig. 1. Large-scale 600 MW power plant model [3].

Suppose the following discrete fuzzy model can be used to present the CCS with both fuzzy inference rules and local state-space models:

$$R^i : IF\ \varphi(k) \in M_i, \quad THEN :$$

$$\begin{cases} x(k+1) = A_i x(k) + B_i u(k) \\ y(k) = C_i x(k) + D_i u(k), \quad i = 1, 2, \ldots, L \end{cases} \tag{1}$$

where R^i denotes the ith fuzzy inference rule, L the number of fuzzy rules, M_i the fuzzy sets, $x(k) \in \Re^n$ the state vector, $u(k) \in \Re^m$ the control input vector, and $y(k) \in \Re^p$ the output vector. The matrices A_i, B_i, C_i, D_i are local system matrices, and $\varphi(k)$ is the antecedent vector of the fuzzy model, which is also the clustering input, composed by current and past measurable variables of the plant.

Let $\omega^i(k)$ be the normalized membership function of the fuzzy set M_i, then the fuzzy model (1) can be expressed in a global form:

$$\begin{cases} x(k+1) = A_\omega x(k) + B_\omega u(k) \\ y(k) = C_\omega x(k) + D_\omega u(k) \end{cases} \tag{2}$$

where $A_\omega = \sum_{i=1}^{L} \omega^i(k) A_i, \quad \omega^i(k) \in [0, 1], \quad \sum_{i=1}^{L} \omega^i(k) = 1$, and other matrices are defined in the similar way.

Modeling of the fuzzy system consists of two parts: the *premise* (structure) design and the *consequence* (local model parameters) design. In this section, we first use the fuzzy clustering to determine the structure of the fuzzy model, i.e., the number of the local models L, and the membership functions ω^i; and then the SID is used to determine the model parameters $\{A_i, B_i, C_i, D_i\}$ through the input/output data of the plant and the corresponding membership functions.

3.1. Premise design using fuzzy clustering

Clustering has been widely accepted as an effective method for designing the premise part of the fuzzy model. It classifies the data according to similarities and organizes the data into groups or clusters. The number of the clusters is corresponding to the number of local models and the clustering centers can be used to calculate the membership functions. A satisfactory clustering can provide an appropriate structure design without much experience on, or nonlinear analysis of the plant.

Before performing the clustering, it is important to select the clustering input vector $\varphi(k)$. For the CCS of power plant, because the dynamics are greatly relying on the power level, throttle pressure as well as the valve positions, the clustering input is chosen as: $\varphi(k) = [E(k-1), P(k-1), u_1(k-1), u_8(k-1)]$ in this paper.

Thus, the data set for clustering, $\overline{X}$, can be constructed as: $\overline{X} = \{X(k) | k = 1, 2. . .\mathrm{N}\}$ with the kth sample $X(k) = [\varphi(k), E(k), P(k)]^T$, where N is the number of the samples. The goal of clustering is then to find L clustering centers V_i, $i = 1, 2, \ldots, L$, such that some measure of the distance between all samples X_k and the cluster centers V_i is minimum.

A modified Gaustafson–Kessel (G–K) clustering algorithm [22] is employed for this purpose, owing to its distinct features such as: local adaptation of the distance metric to the shape of the cluster and relative insensitivity to the data scaling and initialization of the partition matrix defined below.

The G–K clustering is an objective function based clustering, which tries to find L clustering centers V_i, $i = 1, 2, \ldots, L$, and the partition matrix $U = [\mu_{ik}] \in [0, 1]_{L\times N}$ from the data set $\overline{X}$, such that the following objective function is minimum:

$$J(\overline{X}; U, V, A) = \sum_{i=1}^{L}\sum_{k=1}^{N}(\mu_{ik})^m D_{ikA_i}^2 \tag{3}$$

where μ_{ik} is the value of the membership function of the kth sample for the ith fuzzy set in the data set $\overline{X}$, $m \in [1, \infty]$ is a scalar parameter which determines the fuzziness of the resulting clusters, generally set as $m = 2$, and D_{ikA_i} denotes the distance between a sample X_k and a cluster center V_i, which also determines the geometrical shapes of the clustering:

$$D_{ikA_i}^2 = (X_k - V_i)^T A_i (X_k - V_i) \tag{4}$$

in which the positive definite matrix A_i is obtained by:

$$\begin{aligned} A_i &= [\rho_i \det(F_i)]^{1/N} F_i^{-1} \\ F_i &= \frac{\sum_{k=1}^{N}(\mu_{ik})^m (X_k - V_i)(X_k - V_i)^T}{\sum_{k=1}^{N}(\mu_{ik})^m} \end{aligned} \tag{5}$$

As a nonlinear optimization problem, the analytic solutions of the G–K clustering is difficult to obtain; thus an iterative method is used to minimize the objective function, which calculates the cluster centers at the lth iteration by:

$$V_i^{(l)} = \frac{\sum_{k=1}^{N}(\mu_{ik}^{(l-1)})^m X_k}{\sum_{k=1}^{N}(\mu_{ik}^{(l-1)})^m} \tag{6}$$

Then the fuzzy covariance matrix F_i and the distance value D_{ikA_i} can be updated through (5) and (4), and the partition matrix can be determined by:

$$\mu_{ik}^{(l)} = \frac{1}{\sum_{j=1}^{L}(D_{ikA_i}/D_{jkA_j})^{2/(m-1)}} \tag{7}$$

until $||U^{(l)} - U^{(l-1)}|| \le \varepsilon$,which is the termination tolerance. The detailed algorithm can be found in [22].

Once the L clustering centers V_i, $i = 1, 2, \ldots, L$ are obtained, we extract the input centers V_i^{φ} from them, which are set as the centers of the fuzzy set M_i. Then, for a given input vector $\varphi(k)$, a Gaussian-type membership function can be calculated through V_i^{φ}:

$$w^i(k) = \exp\left[-\left(\frac{\left\|\varphi(k) - V_i^{\varphi}\right\|}{\sigma^i}\right)^2\right] \tag{8}$$

where σ^i is the width of the membership function:

$$\sigma^i = \frac{1}{\beta}\left[\frac{1}{j}\sum_{l=1}^{j}\left\|V_i - V_l\right\|\right] \tag{9}$$

with V_l, $l = 1,2,\ldots,j$ being the j closest centers to the *center* V_i. We set $j = 1$ and $\beta = 4$ in this paper and the normalized membership function can be calculated by:

$$\omega^i(k) = \frac{w^i(k)}{\sum_{i=1}^{L} w^i(k)} \tag{10}$$

Thus, we have now successfully developed the premise part of the fuzzy model.

3.2. Consequence design using subspace identification

Considering the global fuzzy model (2), the remaining problem can now be formulated as: given the input sequence $u(k)$, output sequence $y(k)$ and their corresponding membership functions $\omega(k)$ over a time $k = 1, 2, \ldots, N$, find the system matrices A_i, B_i, C_i, and D_i. However, since model (2) is dependent on the membership functions, the global system matrices will be different for different operating point at each time step. This will make the data matrices involved in the SID grow exponentially with the size of the prediction time [32,33], which makes it difficult to implement.

To handle this problem, a simplifying assumption is made that only the input matrices B_i and D_i are dependent on the membership functions, and other matrices except these two, i.e., A and C, are assumed to be independent of the membership functions (e.g., $A_i = A_j = A$, $i, j = 1, 2, \ldots, L$). Under this assumption, the input data can be combined with the membership functions before performing the SID. An approximate fuzzy model is then defined as following:

$$\begin{cases} x(k+1) = Ax(k) + B_\omega u(k) \\ y(k) = Cx(k) + D_\omega u(k) \end{cases} \tag{11}$$

Note that $B_\omega u(k) = \sum_{i=1}^{L} \omega^i(k) B_i u(k) = B[\omega(k) \otimes u(k)]$ and $D_\omega u(k) = \sum_{i=1}^{L} \omega^i(k) D_i u(k) = D[\omega(k) \otimes u(k)]$, where $B = [B_1\, B_2 \ldots B_L]$, $D = [D_1\, D_2 \ldots D_L]$, the membership function vector $\omega(k) = [\omega^1(k)\omega^2(k) \ldots \omega^L(k)]^T$, and $\otimes$ presents the Kronecker product. Model (11) can then be rewritten as:

$$\begin{cases} x(k+1) = Ax(k) + B\mathrm{u}(k) \\ y(k) = Cx(k) + D\mathrm{u}(k) \end{cases} \tag{12}$$

where $\mathrm{u}(k) \equiv \omega(k) \otimes u(k)$ is the *mixed* input resulting from the fuzzy membership functions.

Therefore, by combining the input data with their corresponding membership functions, the standard SID can be extended to find the consequence of the fuzzy model directly. The algorithm of the SID can be found in [23–25] and is not repeated here.

Remark 3.1. This simplification brings a significant advantage in utilizing the SID, although the nonlinear approximation ability of the fuzzy model is not fully utilized. However, since (i) the matrices B_ω, D_ω are dependent on the fuzzy membership functions, through which the input is coupled to the local models; and (ii) the idea of this simplification is consistent with the idea of fuzzy modeling, which is: using the combination of several simple models to approximate the behavior of a complex system; and (iii) if necessary, the accuracy of the model can be improved by further adjusting the number and position of the cluster centers and membership functions, this simplification is reasonable and the resulting model can attain a satisfactory accuracy.

3.3. Summary of the data-driven fuzzy modeling

The whole procedure of the data-driven fuzzy modeling can now be summarized as following:

Step 1: Collect the input–output data of the plant $u(k)$, $y(k)$, $k = 1, 2, \ldots, \mathrm{N}$;
Step 2: Perform the fuzzy clustering to determine the cluster centers V_i and calculate the width of the membership functions σ^i, $i = 1, 2, \ldots, L$, with (9);
Step 3: Calculate the membership function $\omega(k)$ for the input–output data, and calculate the *mixed* input $\mathrm{u}(k) = \omega(k) \otimes u(k)$;
Step 4: Select the maximum order N of the system and build the data Hankel matrices using the output and mixed input data $y(k)$, $\mathrm{u}(k)$, $k = 1, 2, \ldots, \mathrm{N}$;
Step 5: Perform the QR-factorization and the singular value decomposition (SVD) to build the extended observability matrix (system order n, $n \leq N$, is selected during the SVD);
Step 6: Extract the state-space matrices (A, B, C, D) and get the local matrices B_i, D_i, $i = 1, 2, \ldots, L$ from B and D.

Remark 3.2. Compared with the method in [20], the proposed method has the following advantages: (1) the fuzzy model structure and local model identification are strongly linked, thus, the integral fuzzy modeling procedure is simple and direct; (2) division of the whole operation range is determined by the clustering, thus less human intervention is needed; (3) it is more efficient since all local models can be identified together at once; (4) compared with the piecewise linear model in [20], the resulting fuzzy model has smooth transition between local models, thus naturally provides bumpless control.

4. Stable model predictive tracking control

With the fuzzy model obtained in the previous section, various advanced controllers can be designed. To deal with the aforementioned difficulties of the CCS, a stable model predictive tracking controller is proposed in this section.

4.1. Offset-free output tracking

To achieve the offset-free output tracking, a disturbance term $d(k) \in R^{nd}$ is introduced to the fuzzy model (2) to lump the effect of all modeling mismatches and unknown plant variations [26,27]:

$$\begin{cases} x(k+1) = A_\omega x(k) + B_\omega u(k) + E_\omega d(k) \\ y(k) = C_\omega x(k) + D_\omega u(k) + F_\omega d(k) \end{cases} \tag{13}$$

Since the state variables of the identified model and the disturbances are unmeasured, the following fuzzy observer is first designed:

$$\begin{cases} \begin{bmatrix} \hat{x}(k+1) \\ \hat{d}(k+1) \end{bmatrix} = \begin{bmatrix} A_\omega & E_\omega \\ 0 & I \end{bmatrix} \begin{bmatrix} \hat{x}(k) \\ \hat{d}(k) \end{bmatrix} + \begin{bmatrix} B_\omega \\ 0 \end{bmatrix} u(k) + \begin{bmatrix} L_z^1 \\ L_z^2 \end{bmatrix} [\hat{y}(k) - y(k)] \\ \hat{y}(k) = C_\omega \hat{x}(k) + D_\omega u(k) + F_\omega \hat{d}(k) \end{cases} \tag{14}$$

where the symbol "$\wedge$" indicates the estimate. Following the method in [34], we can construct a stable fuzzy observer if there exist matrices H and G_i, and a symmetric positive definite matrix X, such that the following LMI problem is feasible:

$$\begin{bmatrix} H^T + H - X & * \\ HA_i^{aug} + G_i C_i^{aug} & X \end{bmatrix} > 0, \quad i = 1, 2, \ldots, L \tag{15}$$

in which the augmented matrices are defined by

$$A_i^{aug} = \begin{bmatrix} A_i & E_i \\ 0 & I \end{bmatrix}$$

and $C_i^{aug} = [\, C_i \quad F_i \,]$, and "*" in the matrix stands for the corresponding terms in the symmetric matrix. Then the observer gains can be determined by

$$L_i = H^{-1}G_i = [\, L_i^{1^T} \quad L_i^{2^T} \,]^T, \quad i = 1, 2, \ldots, L.$$

Remark 4.1. To ensure the observability of the state variables and disturbance term, the following condition needs to be satisfied:

$$rank \begin{bmatrix} I - A_i & -E_i \\ C_i & F_i \end{bmatrix} = n + nd \tag{16}$$

for all i [26,27].

The disturbance term is then used to construct a steady-state target calculator (SSTC) [26,27] to estimate the equilibrium values of the state and input targets $(x_s(k), u_s(k))$ by solving the following QP problem at each sampling time k:

$$\min_{x_s(k), u_s(k)} (u_s(k) - u_{ref})^T (u_s(k) - u_{ref}) \tag{17}$$

$$s.t.\, x_s(k) = A_\omega x_s(k) + B_\omega u_s(k) + E_\omega \hat{d}(k) \tag{18}$$

$$y_{ref} = C_\omega x_s(k) + D_\omega u_s(k) + F_\omega \hat{d}(k) \tag{19}$$

$$u_{\min} \le u_s(k) \le u_{\max} \tag{20}$$

in which u_{ref} and y_{ref} are desired input and output set points, respectively, and u_{min} and u_{max} are, respectively, the lower and upper limits of the input.

Remark 4.2. If the unknown disturbance would reach a steady-state value asymptotically, the solution results in an offset-free output tracking for the controller [26,27].

Once the optimal steady-state set-point $(x_s(k), u_s(k))$ is obtained, by subtracting (18) and (19) from (13), we can get:

$$\begin{cases} \bar{x}(k+1) = A_\omega \bar{x}(k) + B_\omega \bar{u}(k) + E_\omega \bar{d}(k) \\ \bar{y}(k) = C_\omega \bar{x}(k) + D_\omega \bar{u}(k) + F_\omega \bar{d}(k) \end{cases} \tag{21}$$

where $\bar{x}(k) = x(k) - x_s(k)$, $\bar{u}(k) = u(k) - u_s(k)$, $\bar{y}(k) = y(k) - y_{ref}$ and $\bar{d}(k) = d(k) - \hat{d}(k)$. Noting that the disturbance estimation error $\bar{d}(k)$ is bounded with the help of the observer, we can use the nominal model of (21) as the prediction model:

$$\begin{cases} \bar{x}(k+N+1|k) = A_\omega \bar{x}(k+N|k) + B_\omega \bar{u}(k+N|k) \\ \bar{y}(k+N|k) = C_\omega \bar{x}(k+N|k) + D_\omega \bar{u}(k+N|k) \end{cases} \tag{22}$$

where $N \ge 0$.

4.2. Stable MPC using an output objective function

The stability theory of MPC design has been well established, where an infinite-horizon objective function is adopted and the Lyapunov theory is used to ensure the stability and find the upper-bound of the objective function [14,28–30]. The control input can be solved by minimizing this upper-bound while subjecting to the stability and input constraints in the form of LMIs.

In all of these works a state-variable based objective function

$$J_0^\infty(k) = \sum_{N=0}^{\infty} [\bar{x}^T(k+N|k) Q_0 \bar{x}(k+N|k) + \bar{u}^T(k+N|k) R_0 \bar{u}(k+N|k)] \tag{23}$$

is employed, so that the Lyapunov stability condition can be constructed directly.

For a fuzzy model derived from analytical model, such objective function may easily yield a good performance by tuning of weighting matrices, because the relationship between state and output variables are generally simple [14,28–30]. However, for the subspace identified model, it is difficult to tune the weighting matrices, because the state variables in the model do not have real physical meaning and the relationship between state and output variables are not transparent.

For this reason, we modify the conventional stable MPC by using the output-based objective function:

$$J_0^\infty(k) = \sum_{N=0}^{\infty} [\bar{y}^T(k+N|k) Q_0 \bar{y}(k+N|k) + \bar{u}^T(k+N|k) R_0 \bar{u}(k+N|k)] \tag{24}$$

where $Q_0 = Q_0^T > 0$, $R_0 = R_0^T > 0$ are symmetric positive definite weighting matrices for output and control input, respectively, and we present the following main result:

Theorem 1. *Consider the discrete fuzzy system (13) under input constraint:* $u_{\min} \le u(k+N|k) \le u_{\max}$, $\Delta u_{\min} \le \Delta u(k+N|k) \le \Delta u_{\max}$, $N \ge 0$, *with the fuzzy observer (14) determined by LMIs (15) and steady-state set-points* $(x_s(k), u_s(k))$ *calculated by the SSTC (17)–(20) at sampling time k.*

If there exist N_f *-step free control sequence*

$$\bar{U}(k) = [\bar{u}^T(k|k), \bar{u}^T(k+1|k), \ldots, \bar{u}^T((k+N_f-1|k))]^T \tag{25}$$

matrices Y_i, G, *and symmetric positive definite matrix* $\tilde{S}$, *such that the following LMI problem is feasible:*

$$\begin{array}{ll} \min\limits_{\gamma, \bar{U}(k), Y_i, G, \tilde{S}} & \gamma \\ s.t. & (27)-(30) \end{array} \tag{26}$$

then, at every sampling time k, through minimizing the upper bound of the infinite horizon objective function, γ, *a sequence of free control input,* $u(k+N|k) = \bar{u}(k+N|k) + u_s(k)$, for $0 \le N < N_f$ *and a feedback control law* $u(k+N|k) = Y_\omega G^{-1}\tilde{x}(k+N|k) + u_s(k)$, for $N \ge N_f$ *can be determined by the proposed predictive controller to track the set-points optimally while satisfying input constraints and guaranteeing the input-to-state stability of the closed-loop system:*

where

$$\begin{bmatrix} 1 & * & * & * & * \\ l_x(k)\hat{x}_s(k) + l_u(k)\bar{U}(k) & \frac{\tilde{S}}{2} & 0 & 0 & 0 \\ Q^{1/2}(L_x(k)\hat{x}_s(k) + L_u(k)\bar{U}(k)) & 0 & \frac{\gamma I}{2} & 0 & 0 \\ R^{1/2}\bar{U}(k) & 0 & 0 & \gamma I & 0 \\ l_x(k)w & 0 & 0 & 0 & \frac{\tilde{S}}{2} \end{bmatrix} \ge 0 \tag{27}$$

$$\begin{bmatrix} G + G^T - \tilde{S} & * & * & * \\ (A_i G + B_i Y_i) & \tilde{S} & 0 & 0 \\ Q_0^{1/2}(C_i G + D_i Y_i) & 0 & \gamma I & 0 \\ R_0^{1/2} Y_i & 0 & 0 & \gamma I \end{bmatrix} > 0 \quad i = 1, 2, \ldots, L \tag{28}$$

$$\begin{bmatrix} I_m \\ I_m \\ \vdots \\ I_m \end{bmatrix} (u_{min} - u_s(k)) \le \bar{U}(k) \le \begin{bmatrix} I_m \\ I_m \\ \vdots \\ I_m \end{bmatrix} (u_{max} - u_s(k)) \tag{29}$$

$$\begin{bmatrix} I_m \\ I_m \\ \vdots \\ I_m \end{bmatrix} \Delta u_{\min} \le \zeta \begin{bmatrix} u(k-1) \\ \bar{U}(k) + \begin{bmatrix} I_m \\ I_m \\ \vdots \\ I_m \end{bmatrix} u_s(k) \end{bmatrix} \le \begin{bmatrix} I_m \\ I_m \\ \vdots \\ I_m \end{bmatrix} \Delta u_{\max} \tag{30}$$

in which $Q = I_{N_f} \otimes Q_0$, $R = I_{N_f} \otimes R_0$, w is the upper bound of the state estimation error, $|\tilde{x}| \le w$, $\hat{x}_s(k) = \hat{x}(k) - x_s(k)$ and

$$\zeta = \begin{bmatrix} -I_m & I_m & 0 & \ldots & 0 \\ 0 & -I_m & I_m & \ldots & \vdots \\ \vdots & \vdots & \ddots & \ddots & 0 \\ 0 & \cdots & 0 & -I_m & I_m \end{bmatrix}.$$

Furthermore, to simplify the computation, we assume that the fuzzy model is fixed over the prediction horizon, and the prediction matrices in (27) are given as:

$$l_x(k) = [A_\omega(k)]^{N_f};$$

$$l_u(k) = \begin{bmatrix} [A_\omega(k)]^{N_f-1} & [A_\omega(k)]^{N_f-2} & \ldots & [A_\omega(k)]^0 \end{bmatrix} B_\omega(k);$$

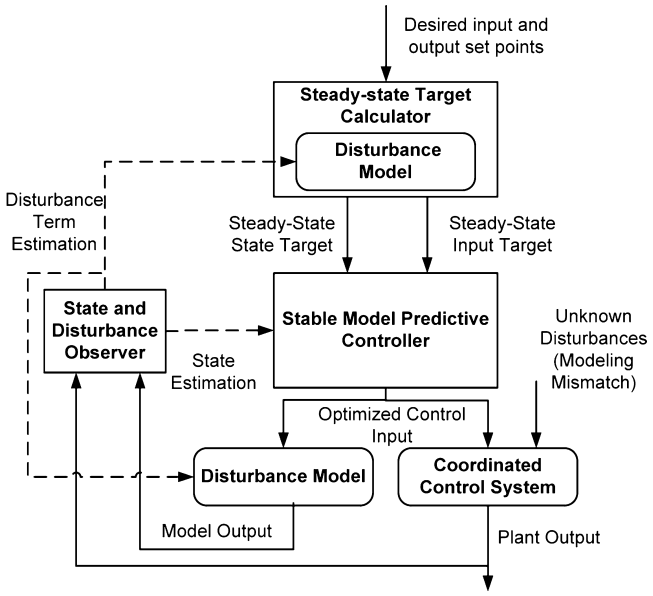

Fig. 2. Working principle of the SMTPC.

$$L_x(k) = \begin{bmatrix} C_\omega(k) \\ C_\omega(k)A_\omega(k) \\ \vdots \\ C_\omega(k)[A_\omega(k)]^{N_f-1} \end{bmatrix};$$

$$L_u(k) = \begin{bmatrix} D_\omega(k) & 0 & \cdots & 0 \\ C_\omega(k)B_\omega(k) & D_\omega(k) & \cdots & 0 \\ \vdots & \ddots & \cdots & 0 \\ C_\omega(k)[A_\omega(k)]^{N_f-2}B_\omega(k) & \cdots & C_\omega(k)B_\omega(k) & D_\omega(k) \end{bmatrix}.$$

The LMI (27) ensures that γ is the upper-bound of the objective function (24), while (28) ensures the input-to-state stability of the closed-loop system, and (29) and (30) respectively give the magnitude and rate constraints for the *free control* sequence (25). The proof of the theorem is given in Appendix A.

The working principle of this SMPTC is shown in Fig. 2. At each sampling time, the first control input $u(k|k)$ in the control sequence is chosen as the current control action to be implemented on the plant.

5. Simulation results

This section demonstrates the data-driven modeling strategy and SMPTC design for the CCS of a power plant. Accuracy of the fuzzy model is demonstrated first, and then the proposed controller are tested and compared with a conventional PI controller and other types of predictive controllers.

5.1. Verification of fuzzy model

The designers of this 600 MW power plant simulator provide an operation range between (600 MW, 2415.5 psig) and (500 MW, 2114.9 psig) for a typical load cycle [3]. In this section, we extend the lower bound to (450 MW, 2000 psig), representing a wide operation range for the power plant, and transitions within this range is considered. In order to overcome the significant nonlinearity and correctly capture the dynamics of the CCS within this operation range, fuzzy modeling technique is utilized and the input sequences shown in Fig. 3 are designed to generate data. The power plant simulator can generate data every 0.1 s, however, such a small sampling rate will focus too much on the identification of noise. Considering both the slow dynamics of fuel flow and the fast dynamics of turbine valve, the sampling time is selected as 1 second and the identified model outputs are shown in Fig. 4, with the number of clusters $L = 6$ and the SID parameter $N = 10$. It can be seen that the resulting fuzzy model has very high precision. The identified TS fuzzy model is given in Appendix B.

A single linear model developed by the SID method using the same data is also tried for comparison; however, due to the high nonlinearity of the plant, it leads to a non-convergent result.

To further test the accuracy of the identified model, another group of data is used for validation as shown in Figs. 5 and 6. The result in Fig. 6 shows that the fuzzy model can capture the CCS dynamics correctly in terms of trend and time constant. The figure also shows a little

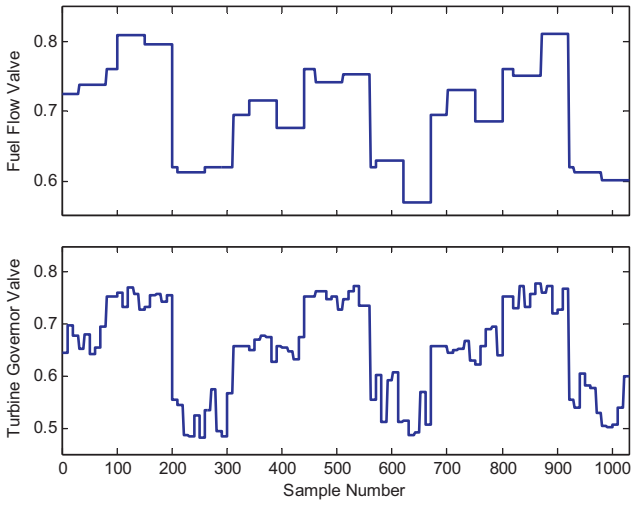

Fig. 3. Input sequences used in the fuzzy model identification.

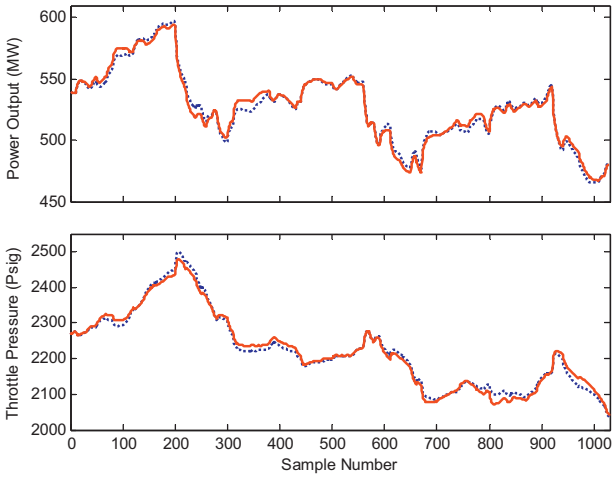

Fig. 4. Fuzzy model identification for the CCS (solid in red: estimated outputs; dotted in blue: real outputs). (For interpretation of the references to color in this figure legend, the reader is referred to the web version of the article.)

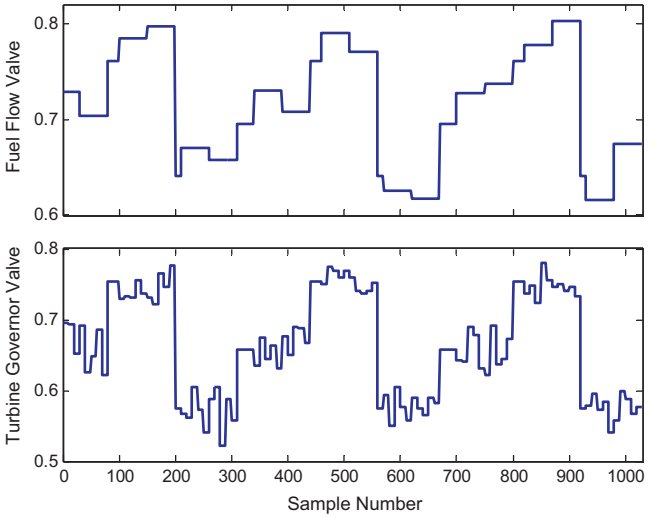

Fig. 5. Input sequences used in the fuzzy model verification.

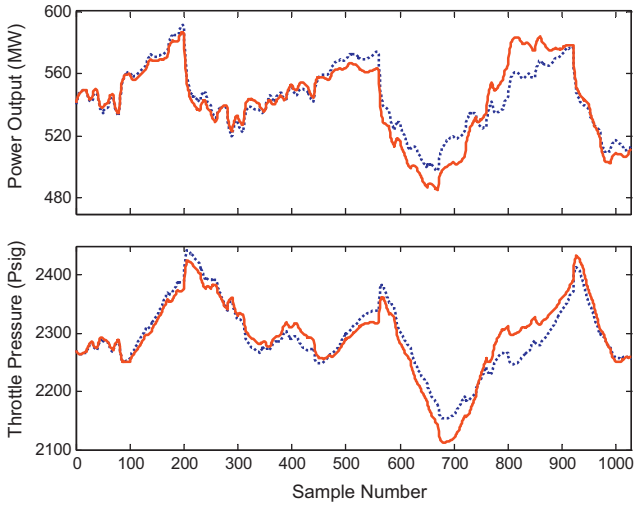

Fig. 6. Fuzzy model verification (solid in red: estimated outputs; dotted in blue: real outputs). (For interpretation of the references to color in this figure legend, the reader is referred to the web version of the article.)

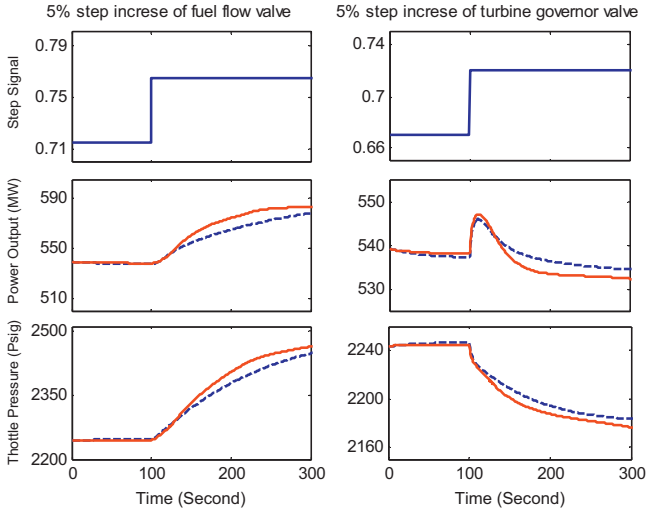

Fig. 7. Open-loop step response test for the CCS of the 600 MW power plant (solid in red: estimated outputs; dashed in blue: real outputs; left column: step response of fuel flow valve u_1, right column: step response of turbine governor valve u_8). (For interpretation of the references to color in this figure legend, the reader is referred to the web version of the article.)

offset between the model output and real output; however, it is acceptable for controller design and can be easily reduced by further tuning of the cluster centers and fuzzy membership functions. The effectiveness of the proposed identification strategy is clearly demonstrated by the results.

At last, we validate the model through open-loop step response tests: 5% step increase for each control valve. The results in Fig. 7 show that the proposed fuzzy model has satisfactory approximation accuracy. The figure also shows the behavior of the CCS, which can be used as useful guide in the controller design:

(1) Turbine governor valve can quickly change the power output; however, since the fuel entering into the unit does not change, the power output will return to the previous level after a while, and what changed is only the stored thermal energy in the unit, as shown in "Throttle Pressure".
(2) Fuel flow valve can change the power output and throttle pressure ultimately; however, this influence has the characteristics of a large inertia.

Comparing with the analytical modeling method, where certain process knowledge is required to derive the model, the proposed approach is more convenient and practical to develop a satisfactory model for a real power plant, and the reasons are below: (a) the employment of Distributed Control Systems (DCS) is now the rule in power plants rather than the exception, thus all the process data are simply collected and archived; (b) once the experiment is approved, the power plant can be separated from the grid. Then with the help of operators who well understand the dynamics of the plant, it is not difficult to design and run the experiment to obtain sufficient qualified data without putting the plant under too much stress; (c) the closed-loop subspace identification theory has been developing fast recently [25], which can be directly used in our method instead of the regular SID algorithm. Therefore, even if the open-loop experiment is not allowed, it is still possible to develop the model through the closed-loop system data.

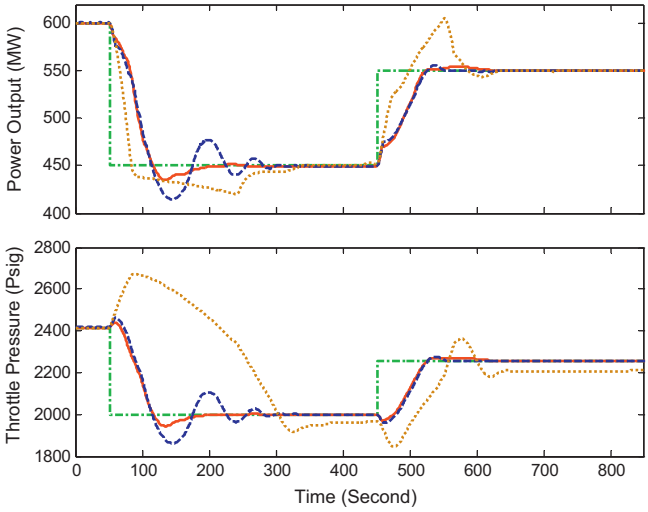

Fig. 8. Performance of the CCS for a 600–450–550 MW load variation: output variables (solid in red: SMPTC; dashed in blue: MPC; dotted in brown: PI; dot-dashed in green: reference). (For interpretation of the references to color in this figure legend, the reader is referred to the web version of the article.)

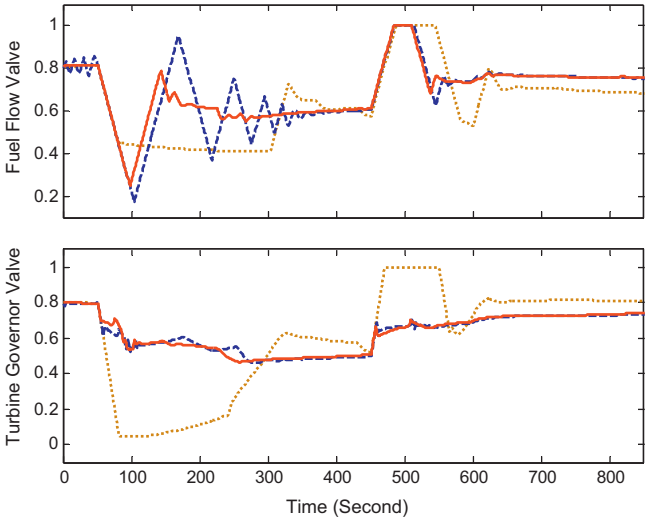

Fig. 9. Performance of the CCS for a 600–450–550 MW load variation: manipulated variables (solid in red: SMPTC; dashed in blue: MPC; dotted in brown: PI). (For interpretation of the references to color in this figure legend, the reader is referred to the web version of the article.)

5.2. Testing of the SMPTC

In this section, the proposed SMPTC is applied to the CCS of the 600 MW power plant and used as the primary controller to track the expected operating points of output power and throttle pressure. At the same time, a set of feedforward–feedback PI controllers are used as sub-controllers to manipulate all other valves shown in Fig. 1 to maintain fuel–air-ratio, furnace pressure, Superheater/Reheater temperature, drum water level, and so on.

The sampling time of the SMPTC is set as 1 s, and we set: $E_i = [0.01,0.1;0.01,0.002;0.5,0.08;0.01,0.02]$, $F_i = [0]_{2\times 2}$, $i = 1, \ldots, 6$, for the disturbance matrices. The tuning of them will influence the disturbance rejection property of the controller, and how to determine them are introduced well in [26,27]. For the parameters of the SMPTC, N_f is the number of free control inputs and tuning of it is a trade-off between control performance and computational burden; Q_0 and R_0 are weighting matrices of outputs and control moves, respectively, thus tuning of them is a trade-off between output set-point tracking performance and input set-point tracking performance. The selection for the state estimation error w will influence the feasibility of the SMPTC and the initial status of the control system. These parameters are set as: $N_f = 10$; $Q_0 = diag(120,10)$; $R_0 = 1000 \times diag(1,1)$; $w = [1,1,1,1]^T$ in this simulation. The input constraints are $u_{1,8,max} = 1$; $u_{1,8,min} = 0$ and $\Delta u_{1,max} = 0.012$; $\Delta u_{1,min} = -0.012$; $\Delta u_{8,max} = 0.024$; $\Delta u_{8,min} = -0.024$ due to the physical limitations of the valves.

The first case is designed to show the overall performance of the controllers over a wide operation range. At $t = 50$ s, the set-points of power output and throttle pressure change from (600 MW, 2415.5 psig) to (450 MW, 2000 psig), then at $t = 450$ s change to (550 MW, 2257.4 psig).

Two other controllers are used for comparison:

(1) Regular MPC [16] built on the proposed fuzzy model with the same Q_0, R_0 and sampling time, the prediction and control horizon parameters are set as: $N_p = N_c = 10$ (MPC);

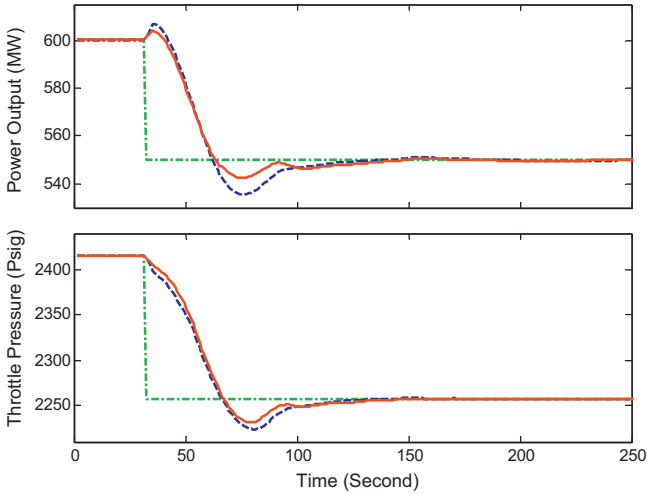

Fig. 10. Performance of the CCS for a 600–550 MW load variation: output variables (solid in red: SMPTC; dashed in blue: SMPTC_linear; dot-dashed in green: reference). (For interpretation of the references to color in this figure legend, the reader is referred to the web version of the article.)

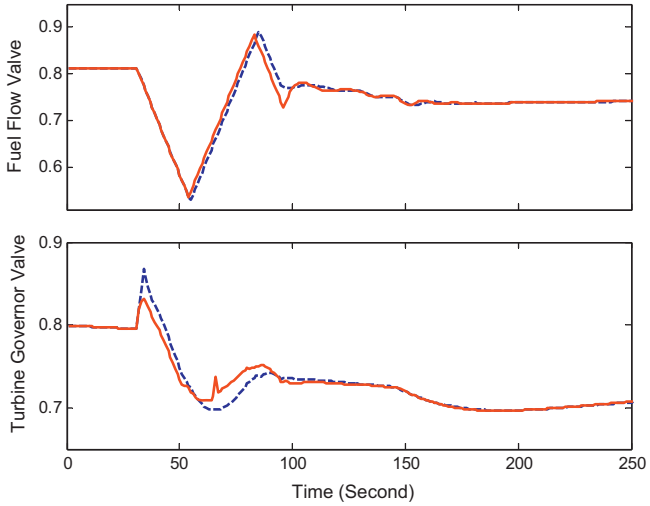

Fig. 11. Performance of the CCS for a 600–550 MW load variation: manipulated variables (solid in red: SMPTC; dashed in blue: SMPTC_linear). (For interpretation of the references to color in this figure legend, the reader is referred to the web version of the article.)

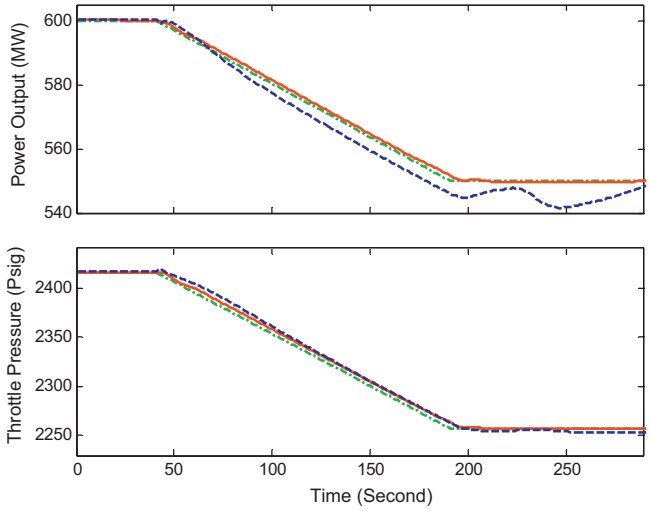

Fig. 12. Performance of the CCS for a 600–550 MW load variation: output variables (solid in red: SMPTC; dashed in blue: SMPTC_state; dot-dashed in green: reference). (For interpretation of the references to color in this figure legend, the reader is referred to the web version of the article.)

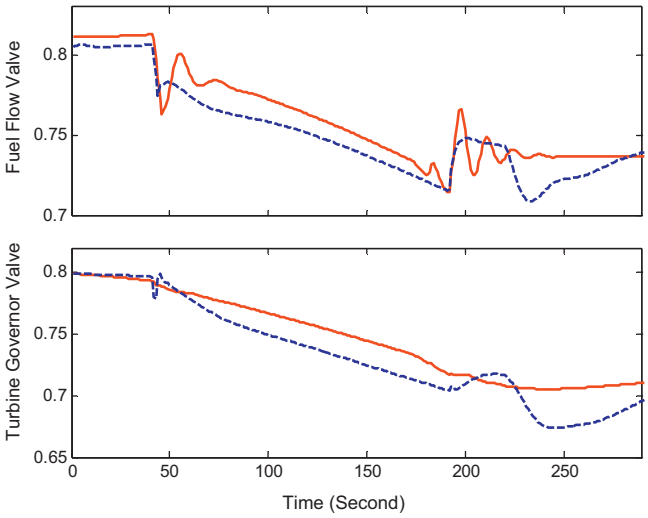

Fig. 13. Performance of the CCS for a 600–550 MW load variation: manipulated variables (solid in red: SMPTC; dashed in blue: SMPTC_state). (For interpretation of the references to color in this figure legend, the reader is referred to the web version of the article.)

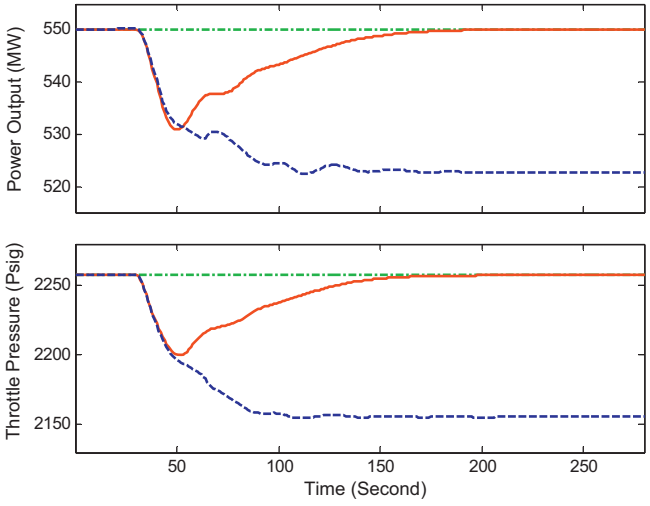

Fig. 14. Performance of the CCS at 550 MW operating point, an unknown input disturbance $u_{1,d} = -0.2$occurs at $t = 30$ s: output variables (solid in red: SMPTC; dashed in blue: SMPC; dot-dashed in green: reference). (For interpretation of the references to color in this figure legend, the reader is referred to the web version of the article.)

(2) Feedforward–feedback PI controllers originally installed in the plant simulator (PI). The controller is designed based on the coordinated boiler-following mode and the parameters are optimized and fixed under 600 MW operating condition.

The simulation results in Figs. 8 and 9 show that the proposed SMPTC has the best performance, which can quickly track the power and pressure set-points in a wide range. Based on the same fuzzy model, the MPC also has a good performance; however, it cannot guarantee the stability of the closed-loop system, thus for the given short predictive horizon, the result shows a little oscillation during the transition between 600 MW and 450 MW. For the PI controller under the boiler-following mode, the governor valve is used to regulate the power output and the fuel flow valve is used to regulate the throttle pressure. Although the feedforward action accelerates the response of the controller and the parameters are well tuned at a given loading condition, the PI controller has drawbacks: (a) the separate single-input, single-output (SISO) loops do not account for the interactions of the different thermal properties in the plant; (b) the controller parameters are fixed, thus are no longer suited when wide range load following operation is required and the nonlinearity of the plant become significant; and (c) the controller cannot handle the constraints of manipulated variables in the controller calculation stage. Thus its performance is decreased when physical limitations of the valves in plants are involved, which may also cause the integral windup (can be viewed around $t = 500$ s: the power output has already exceeded the set-point, but the governor valve keeps fully open). Therefore, it is difficult to achieve a satisfactory control for both power and pressure, and the performance is degraded over a wide operation range.

Note that the QP based SSTC and LMI based stable MPC are both computationally efficient. For the proposed SMPTC, the SSTC calculation takes 0.0771 s and the controller calculation takes 0.5188 s for each step during the simulation. (MATLAB R2006a is used on our PC: 2.00 GHz Core-i7 CPU, 8 G Memory)

To further test the effectiveness of the fuzzy model based controller, a same SMPTC based on a single linear model identified around the 570–580 MW operating region (SMPTC_linear) is compared with the proposed controller. The simulation is made considering a set-points change from (600 MW, 2415.5 psig) to (550 MW, 2257.4 psig) and the results are shown in Figs. 10 and 11. The proposed fuzzy SMPTC can achieve a better control performance.

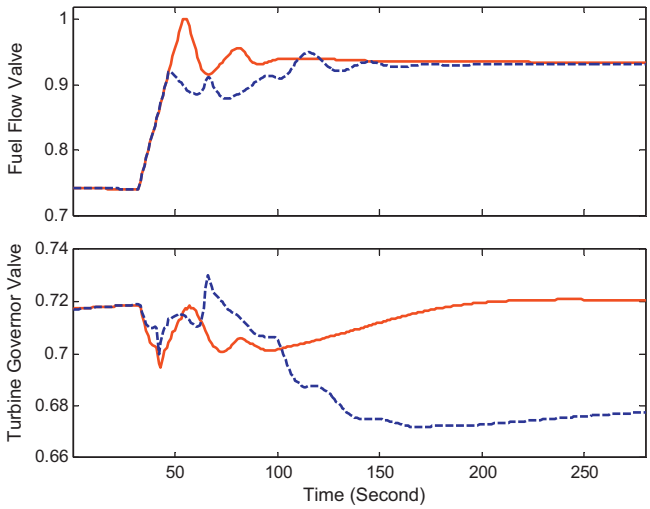

Fig. 15. Performance of the CCS at 550 MW operating point, an unknown input disturbance $u_{1,d} = -0.2$ occurs at $t = 30$ s: manipulated variables (solid in red: SMPTC; dashed in blue: SMPC). (For interpretation of the references to color in this figure legend, the reader is referred to the web version of the article.)

Then we compare the proposed controller with conventional SMPTC using the state-variable based objective function (23) (SMPTC_state). A linearly decreasing load is considered such that at $t = 40$ s, the power set-point decreases from 600 MW to 550 MW in the rate of 0.333 MW/s and the pressure set-point decreases from 2415.5 psig to 2257.4 psig in the rate of 1.054 psig/s. For the SMPTC_state, we set $Q_0 = 0.01 \times diag(1,1,3,1)$; $R_0 = diag(1,1)$, other parameters are set the same as for the SMPTC and the simulation results are shown in Figs. 12 and 13. Due to the reason we discussed in Section 4, it is difficult to find the weighting matrices for the SMPTC_state to attain a satisfactory tracking of the set-points. Moreover, since the dimension of the state vector is $n = 4$ in our case, which is twice as much as the output dimension, the computational burden of SMPC_state is also much heavier.

At last, we test the proposed controller under significant unknown disturbances. We assume that the plant is working at 550 MW operation point, and at $t = 30$ s an unknown input disturbance $u_{1,d} = -0.2$ is acted on the fuel flow due to the wear and tear of the valve. The proposed controller is compared with the same controller without using the disturbance model and SSTC (SMPC) as shown in Figs. 14 and 15.

The result shows that the proposed SMPTC handles the unknown plant disturbances effectively and keeps the plant operating in an expected condition. However, for the SMPC, since the state and input set-points are fixed at certain load level, significant control offset occurs in the case of unknown plant disturbances.

6. Conclusion

The cooperation of fuzzy model and predictive control provides an effective way to overcome the control problem of the large-scale power plant. A TS-fuzzy model is first developed based on the fuzzy clustering and subspace identification method. The resulting model is shown to represent the CCS dynamics very closely and is well suited for controller design due to its state-space structure, and thus, an SMPTC is proposed on this fuzzy model. An output-based objective function is used in the controller formulation to make it applicable for the data-driven model. With the help of the state and disturbance observer and SSTC, the proposed controller can achieve a tracking control of the CCS while satisfying the input constraints and guaranteeing the input-to-state stability of the system even in the case of significant unknown disturbances or plant parameter variations. The advantages and effectiveness of the proposed modeling and controller design are demonstrated through the simulations of a large-scale 600 MW power plant.

Acknowledgements

The authors acknowledge the National Natural Science Foundation of China (NSFC) under Grant 51476027 and Grant 51036002, the Doctoral Fund of the Ministry of Education of China under Grant 20130092110061, the Natural Science Foundation of Jiangsu Province, China under Grant BK20141119, the Foundation of State Key Laboratory of Coal Combustion under Grant FSKLCC1203 for funding this work.

Appendix A.

A.1. Proof of Theorem 1

Part 1: Minimizing the upper bound of infinite-horizon objective function

To guarantee the stability of the closed-loop system on the infinite-time horizon, state-feedback control law has to be used. This also provides a way to convert the problem of calculating infinite number of control inputs (actually infeasible) into that of finding a control law (feasible). However, the format of the feedback law greatly limits the optimality of the MPC, which is first shown in [29], thus the first finite number of control inputs (which are obviously more important than the future ones) are separated from the rest of the inputs in feedback form and set as the free control variables as in the regular MPC.

This division improves the optimality of SMPC at the expense of computational burden. In this paper, the first N_f number of control inputs are set aside as free. Corresponding to this division, the infinite-horizon objective function (24) is also divided into two parts [29,30]:

$$J_0^{\infty}(k) = J_0^{N_f-1}(k) + J_{N_f}^{\infty}(k) \tag{A1}$$

where

$$J_0^{N_f-1}(k) = \sum_{N=0}^{N_f-1} [\bar{y}^T(k+N|k)Q_0\bar{y}(k+N|k) + \bar{u}^T(k+N|k)R_0\bar{u}(k+N|k)] = (L_x(k)\bar{x}(k) + L_u(k)\bar{U}(k))^T Q(L_x(k)\bar{x}(k) + L_u(k)\bar{U}(k)) + \bar{U}(k)^T R\bar{U}(k)$$

$$J_{N_f}^{\infty}(k) = \sum_{N=N_f}^{\infty} [\bar{y}^T(k+N|k)Q_0\bar{y}(k+N|k) + \bar{u}^T(k+N|k)R_0\bar{u}(k+N|k)]$$

Suppose a common Lyapunov function (CLF) [28,29],

$$V(x) = \bar{x}^T S^{-1}\bar{x} \tag{A2}$$

satisfies:

$$\Delta V(k) = \bar{x}(k+1)^T S^{-1}\bar{x}(k+1) - \bar{x}(k)^T S^{-1}\bar{x}(k) < 0 \tag{A3}$$

for all time, the system is guaranteed to be stable in the sense of Lyapunov.

To find the upper bound of the infinite-horizon objective function (24), suppose the CLF satisfies:

$$V(k+N+1|k) - V(k+N|k) < -[\bar{y}(k+N|k)^T Q_0\bar{y}(k+N|k) + \bar{u}(k+N|k)^T R_0\bar{u}(k+N|k)] \tag{A4}$$

Summing (A4) for $N = N_f$ to $N = \infty$, and with $\bar{x}(\infty|k) = 0$ and $V(\infty|k) = 0$, we get:

$$J_{N_f}^{\infty}(k) < V(k+N_f|k) = \bar{x}(k+N_f|k)^T S^{-1}\bar{x}(k+N_f|k) = (l_x(k)\bar{x}(k) + l_u(k)\bar{U}(k))^T S^{-1}(l_x(k)\bar{x}(k) + l_u(k)\bar{U}(k)) \tag{A5}$$

Thus we can get the upper bound of $J_0^{\infty}(k)$:

$$J_0^{\infty}(k) = J_0^{N_f-1}(k) + J_{N_f}^{\infty}(k) < (L_x(k)\bar{x}(k) + L_u(k)\bar{U}(k))^T Q(L_x(k)\bar{x}(k) + L_u(k)\bar{U}(k)) + \bar{U}(k)^T R\bar{U}(k) + (l_x(k)\bar{x}(k) + l_u(k)\bar{U}(k))^T S^{-1}(l_x(k)\bar{x}(k) + l_u(k)\bar{U}(k)) \tag{A6}$$

However, in (A6), $\bar{x}(k) = x(k) - x_s(k)$ is unmeasured, thus we express it as:

$$\bar{x}(k) = \hat{x}(k) + \tilde{x}(k) - x_s(k) = \hat{x}_s(k) + \tilde{x}(k) \tag{A7}$$

where $\tilde{x}(k)$ is the estimation error between $x(k)$ and $\hat{x}(k)$, and $\hat{x}_s(k) = \hat{x}(k) - x_s(k)$ is the estimated shifted state-variables.

Then we have, the first term on the right hand of (A6):

$$= (L_x(k)\hat{x}_s(k) + L_u(k)\bar{U}(k) + L_x(k)\tilde{x}(k))^T Q(L_x(k)\hat{x}_s(k) + L_u(k)\bar{U}(k) + L_x(k)\tilde{x}(k)) \le 2(L_x(k)\hat{x}_s(k) + L_u(k)\bar{U}(k))^T Q(L_x(k)\hat{x}_s(k) + L_u(k)\bar{U}(k)) + 2(L_x(k)\tilde{x}(k))^T Q(L_x(k)\tilde{x}(k))$$

Consider that the estimation error is bounded with the help of the observer: $|\tilde{x}(k)| \le w$.

$$2(L_x(k)\tilde{x}(k))^T Q(L_x(k)\tilde{x}(k)) \le 2(L_x(k)w)^T Q(L_x(k)w) = c$$

in which c is a constant. Thus we further have:

The first term on the right hand of (A6)≤

$$2(L_x(k)\hat{x}_s(k) + L_u(k)\bar{U}(k))^T Q(L_x(k)\hat{x}_s(k) + L_u(k)\bar{U}(k)) + c \tag{A8}$$

Similarly, the third term on the right hand of (A6)

$$= (l_x(k)\hat{x}_s(k) + l_u(k)\bar{U}(k) + l_x(k)\tilde{x}(k))^T S^{-1}(l_x(k)\hat{x}_s(k) + l_u(k)\bar{U}(k) + l_x(k)\tilde{x}(k)) \le 2(l_x(k)\hat{x}_s(k) + l_u(k)\bar{U}(k))^T S^{-1}(l_x(k)\hat{x}_s(k) + l_u(k)\bar{U}(k)) + 2(l_x(k)w)^T S^{-1}(l_x(k)w) \tag{A9}$$

Substituting (A8) and (A9) into (A6), we can get:

$$J_0^{\infty}(k) \le c + \bar{U}(k)^T R\bar{U}(k) + 2(l_x(k)w)^T S^{-1}(l_x(k)w) + 2(L_x(k)\hat{x}_s(k) + L_u(k)\bar{U}(k))^T Q(L_x(k)\hat{x}_s(k) + L_u(k)\bar{U}(k)) + 2(l_x(k)\hat{x}_s(k) + l_u(k)\bar{U}(k))^T S^{-1}(l_x(k)\hat{x}_s(k) + l_u(k)\bar{U}(k)) \tag{A10}$$

Define a scalar γ and suppose:

$$\bar{U}(k)^T R\bar{U}(k) + 2(l_x(k)w)^T S^{-1}(l_x(k)w) + 2(L_x(k)\hat{x}_s(k) + L_u(k)\bar{U}(k))^T Q(L_x(k)\hat{x}_s(k) + L_u(k)\bar{U}(k)) + 2(l_x(k)\hat{x}_s(k) + l_u(k)\bar{U}(k))^T S^{-1}(l_x(k)\hat{x}_s(k) + l_u(k)\bar{U}(k)) \le \gamma \tag{A11}$$

Then minimizing the upper bound of $J_0^{\infty}(k)$ is equivalent to the minimization of γ, subject to (A11).
By defining $\tilde{S}^{-1} = \gamma^{-1}S^{-1}$, and using the Schur complements [28], (A11) can be expressed as (27) in the form of LMI.

Part 2: stability constraint

Using the state feedback control law:

$$\tilde{u}(k+N) = Y_\omega G^{-1}\tilde{x}(k+N|k), \quad N \geq N_f \tag{A12}$$

the nominal predictive closed-loop fuzzy system (22) can be described as:

$$\tilde{x}(k+N+1|k) = (A_\omega + B_\omega Y_\omega G^{-1})\tilde{x}(k+N|k) \tag{A13}$$

$$\tilde{y}(k+N|k) = (C_\omega + D_\omega Y_\omega G^{-1})\tilde{x}(k+N|k) \tag{A14}$$

Substituting (A12)–(A14) into (A4) and noting the fact that:

$$(G-\tilde{S})^T\tilde{S}^{-1}(G-\tilde{S}) > 0 \Rightarrow G^T\tilde{S}^{-1}G \geq G^T + G - \tilde{S} \tag{A15}$$

then the stability constraint (A4) is satisfied if the following holds:

$$G^T + G - \tilde{S} - (A_iG + B_iY_i)^T\tilde{S}^{-1}(A_iG + B_iY_i) - (C_iG + D_iY_i)^TQ_0\gamma^{-1}(C_iG + D_iY_i) - Y_i^TR_0\gamma^{-1}Y_i > 0, \quad i = 1, 2, \ldots, L \tag{A16}$$

which can be expressed by the LMIs (28).

Part 3: input constraint

Since the control sequence is divided into free control inputs and controls in state feedback law, appropriate input constraints have to be given. Because the free control inputs are the same as in the regular MPC, constraints (28) and (29) can be directly used for the magnitude and rate constraints. However, for the state feedback law, it is difficult to give the magnitude and rate constraints simultaneously while guaranteeing the stability. Therefore, since we have already constrained the first N_f control inputs, we ignore the constraints for the future controls in state feedback form so that the stability will be maintained.

Remark A.1. The use of the CLF results in some conservatism in the stability design, because it requires to find a common Lyapunov matrix for all local models. This conservatism can be relaxed by adopting advanced Lyapunov functions, such as piecewise Lyapunov function (PLF) [30], fuzzy Lyapunov function (FLF) or extended-FLF [14] at the expense of increasing the number of LMIs. Modified controllers are easily derived following the same procedure. Considering both the control performance and computation requirement, the CLF is chosen to design the SMPTC for the CCS in this paper.

Appendix B. TS fuzzy model for the CCS of 600 MW power plant

R^1 : *IF* $\varphi_k \in M_1$ ($V_1^{\varphi} = (538.2186, 2205.4587, 0.7303, 0.7173)$, $\sigma_1 = 8.2369$),

THEN :

$$\begin{cases} x_{k+1} = \begin{bmatrix} 0.9945 & -0.0233 & 0.0202 & -0.0172 \\ 0.0038 & 0.8179 & 0.1737 & 0.1178 \\ -0.0013 & .0872 & 0.9043 & 0.0244 \\ 0.0031 & -0.0334 & 0.0172 & 0.9554 \end{bmatrix} x_k + \begin{bmatrix} -3.5389 & 5.7488 \\ 4.0675 & 31.9474 \\ -3.9890 & -15.9638 \\ 7.6927 & 0.9500 \end{bmatrix} u_k \\ y_k = \begin{bmatrix} -1.0393 & 1.4309 & -0.2366 & -0.6886 \\ -6.3265 & -102273 & 0.9308 & -0.3063 \end{bmatrix} x_k + \begin{bmatrix} -2.6987 & 8.8412 \\ -1.9223 & -7.0063 \end{bmatrix} u_k; \end{cases}$$

R^2 : *IF* $\varphi_k \in M_2$($V_2^{\varphi} = (527.9369, 2390.7844, 0.6166, 0.5194)$, $\sigma_2 = 15.2262$),

THEN :

$$\begin{cases} x_{k+1} = \begin{bmatrix} 0.9945 & -0.0233 & 0.0202 & -0.0172 \\ 0.0038 & 0.8179 & 0.1737 & 0.1178 \\ -0.0013 & .0872 & 0.9043 & 0.0244 \\ 0.0031 & -0.0334 & 0.0172 & 0.9554 \end{bmatrix} x_k + \begin{bmatrix} -3.1464 & 5.2100 \\ 1.3818 & 34.7329 \\ 0.4601 & -20.3296 \\ 5.0709 & 3.4278 \end{bmatrix} u_k \\ y_k = \begin{bmatrix} -1.0393 & 1.4309 & -0.2366 & -0.6886 \\ -6.3265 & -102273 & 0.9308 & -0.3063 \end{bmatrix} x_k + \begin{bmatrix} -6.6482 & 12.8909 \\ -8.9934 & -1.4153 \end{bmatrix} u_k; \end{cases}$$

R^3 : *IF* $\varphi_k \in M_3\,(V_3^{\varphi} = (491.5588, 2174.0543, 0.6152, 0.5516),\ \sigma_3 = 14.0611)$,

THEN :

$$\begin{cases} x_{k+1} = \begin{bmatrix} 0.9945 & -0.0233 & 0.0202 & -0.0172 \\ 0.0038 & 0.8179 & 0.1737 & 0.1178 \\ -0.0013 & .0872 & 0.9043 & 0.0244 \\ 0.0031 & -0.0334 & 0.0172 & 0.9554 \end{bmatrix} x_k + \begin{bmatrix} -3.3749 & 5.6302 \\ 2.1319 & 33.7359 \\ -9.6061 & -9.5058 \\ 12.0482 & -4.0718 \end{bmatrix} u_k \\ y_k = \begin{bmatrix} -1.0393 & 1.4309 & -0.2366 & -0.6886 \\ -6.3265 & -102273 & 0.9308 & -0.3063 \end{bmatrix} x_k + \begin{bmatrix} -3.5892 & 8.6422 \\ -8.6666 & -2.5654 \end{bmatrix} u_k; \end{cases}$$

R^4 : *IF* $\varphi_k \in M_4\ \ (V_4^{\varphi} = (519.5093, 2108.4673, 0.7474, 0.7047), \sigma_4 = 17.8237)$,

THEN :

$$\begin{cases} x_{k+1} = \begin{bmatrix} 0.9945 & -0.0233 & 0.0202 & -0.0172 \\ 0.0038 & 0.8179 & 0.1737 & 0.1178 \\ -0.0013 & .0872 & 0.9043 & 0.0244 \\ 0.0031 & -0.0334 & 0.0172 & 0.9554 \end{bmatrix} x_k + \begin{bmatrix} -2.7790 & 4.8989 \\ 4.3101 & 31.5112 \\ -4.5815 & -14.5272 \\ 7.3704 & 0.4806 \end{bmatrix} u_k \\ y_k = \begin{bmatrix} -1.0393 & 1.4309 & -0.2366 & -0.6886 \\ -6.3265 & -102273 & 0.9308 & -0.3063 \end{bmatrix} x_k + \begin{bmatrix} -3.0935 & 6.9652 \\ -12.9523 & 4.4722 \end{bmatrix} u_k; \end{cases}$$

R^5 : *IF* $\varphi_k \in M_5 (V_5^{\varphi} = (568.6231, 2345.4637, 0.7716, 0.7168),\ \sigma_5 = 15.2262)$,

THEN :

$$\begin{cases} x_{k+1} = \begin{bmatrix} 0.9945 & -0.0233 & 0.0202 & -0.0172 \\ 0.0038 & 0.8179 & 0.1737 & 0.1178 \\ -0.0013 & .0872 & 0.9043 & 0.0244 \\ 0.0031 & -0.0334 & 0.0172 & 0.9554 \end{bmatrix} x_k + \begin{bmatrix} -3.3550 & 5.4969 \\ 2.5740 & 33.4784 \\ -2.8989 & -16.9505 \\ 6.8917 & 1.4960 \end{bmatrix} u_k \\ y_k = \begin{bmatrix} -1.0393 & 1.4309 & -0.2366 & -0.6886 \\ -6.3265 & -102273 & 0.9308 & -0.3063 \end{bmatrix} x_k + \begin{bmatrix} -6.0665 & 12.3414 \\ -9.7702 & 0.1015 \end{bmatrix} u_k; \end{cases}$$

R^6 : *IF* $\varphi_k \in M_6\ \ (V_6^{\varphi} = (536.1901, 2238.3435, 0.7023, 0.6639), \sigma_6 = 8.2369)$,

THEN :

$$\begin{cases} x_{k+1} = \begin{bmatrix} 0.9945 & -0.0233 & 0.0202 & -0.0172 \\ 0.0038 & 0.8179 & 0.1737 & 0.1178 \\ -0.0013 & .0872 & 0.9043 & 0.0244 \\ 0.0031 & -0.0334 & 0.0172 & 0.9554 \end{bmatrix} x_k + \begin{bmatrix} -3.1915 & 5.4035 \\ 2.7761 & 33.0922 \\ -5.3061 & -14.3542 \\ 9.2393 & -0.8768 \end{bmatrix} u_k \\ y_k = \begin{bmatrix} -1.0393 & 1.4309 & -0.2366 & -0.6886 \\ -6.3265 & -102273 & 0.9308 & -0.3063 \end{bmatrix} x_k + \begin{bmatrix} -3.2361 & 9.2342 \\ -7.3239 & -2.5430 \end{bmatrix} u_k \end{cases}$$

References

[1] S. Li, H. Liu, W.J. Cai, Y.C. Soh, L.H. Xie, A new coordinated control strategy for boiler–turbine system of coal-fired power plant, IEEE Trans. Control Syst. Technol. 13 (November) (2005) 943–954.
[2] R. Garduno-Ramirez, K.Y. Lee, Wide-range operation of a power unit via feedforward fuzzy control, IEEE Trans. Energy Convers. 15 (December (4)) (2000) 421–426.
[3] J.S. Heo, K.Y. Lee, R. Garduno-Ramirez, Multiobjective control of power plant using particle swarm optimization techniques, IEEE Trans. Energy Convers. 21 (June (2)) (2006) 552–561.
[4] S. Zhang, C.W. Taft, J. Bentsman, A. Hussey, B. Petrus, Simultaneous gains tuning in boiler/turbine PID-based controller clusters using iterative feedback tuning methodology, ISA Trans. 51 (September) (2012) 609–621.
[5] W. Tan, H.J. Marquez, T. Chen, J. Liu, Analysis and control of a nonlinear boiler–turbine unit, J. Process Control 15 (December) (2005) 883–891.
[6] P. Chen, J. Shamma, Gain-scheduled l^1-optimal control for boiler–turbine dynamics with actuator saturation, J. Process Control 3 (April) (2004) 263–277.
[7] K. Zheng, J. Bentsman, C.W. Taft, Full operating range robust hybrid control of a coal-fired boiler/turbine unit, J. Dyn. Syst. Meas. Control 130 (July) (2008) 041011-1–041011-14.
[8] J. Wu, S.K. Nguang, J. Shen, G. Liu, Y. Li, Robust H_∞ tracking control of boiler–turbine systems, ISA Trans. 49 (July) (2010) 369–375.
[9] U. Moon, K.Y. Lee, A boiler–turbine system control using a fuzzy auto-regressive moving average (FARMA) model, IEEE Trans. Energy Convers. 18 (March (1)) (2003) 142–148.
[10] R. Dimeo, K.Y. Lee, Boiler–turbine control system design using a genetic algorithm, IEEE Trans. Energy Convers. 10 (December) (1995) 752–759.
[11] U. Moon, K.Y. Lee, Step-response model development for dynamic matrix control of a drum-type boiler–turbine system, IEEE Trans. Energy Convers. 24 (June) (2009) 423–430.
[12] K.Y. Lee, J.H. Van Sickel, J.A. Hoffman, W.-H. Jung, S.-H. Kim, Controller design for a large-scale ultrasupercritical once-through boiler power plant, IEEE Trans. Energy Convers. 25 (December (4)) (2010) 1063–1070.
[13] X. Liu, P. Guan, C.W. Chan, Nonlinear multivariable power plant coordinate control by constrained predictive scheme, IEEE Trans. Control Syst. Technol. 18 (September (5)) (2010) 1116–1125.
[14] X. Wu, J. Shen, Y. Li, K.Y. Lee, Stable model predictive control based on TS fuzzy model with application to boiler–turbine coordinated system, in: Proc. 50th IEEE Conference on Decision and Control, December, 2011, pp. 3356–3361.
[15] Y. Li, J. Shen, K.Y. Lee, X. Liu, Offset-free fuzzy model predictive control of a boiler–turbine system based on genetic algorithm, Simul. Modell. Pract. Theory 26 (August) (2012) 77–95.

[16] K. Wu, T. Zhang, J. Lv, W. Xiang, Model predictive control for nonlinear boiler–turbine system based on fuzzy gain scheduling, in: Proc. 2008 IEEE International Conference on Automation and Logistics, September, 2008, pp. 1115–1120.
[17] J. Wu, J. Shen, M. Krug, S.K. Nguang, Y. Li, GA-based nonlinear predictive switching control for a boiler–turbine system, J. Control Theory Appl. 10 (July (1)) (2012) 100–106.
[18] X.J. Liu, X.B. Kong, Nonlinear fuzzy model predictive iterative learning control for drum-type boiler–turbine system, J. Process Control 23 (8) (2013) 1023–1040.
[19] X.J. Liu, C.W. Chan, Neuro-fuzzy generalized predictive control of boiler steam temperature, IEEE Trans. Energy Convers. 21 (4) (2006) 900–908.
[20] X. Wu, J. Shen, Y. Li, K.Y. Lee, Data-driven modeling and control for boiler–turbine unit, IEEE Trans. Energy Convers. 28 (3) (Sep. 2013) 470–481.
[21] T. Takagi, M. Sugeno, Fuzzy identification of systems and its application to modeling and control, IEEE Trans. Syst. Man Cybern. 15 (January–February) (1985) 116–132.
[22] R. Babuska, P.J. van de Veen, U. Kaymak, Improved covariance estimation for Gustafson–Kessel clustering, in: Proc. 2002 IEEE International Conference on Fuzzy System, May, 2002, pp. 1081–1085.
[23] P.V. Overschee, B.D. Moor, A unifying theorem for three subspace system identification algorithms, Automotica 31 (December (12)) (1995) 1853–1861.
[24] W. Favoreel, B.D. Moor, P.V. Overschee, Subspace state space system identification for industrial processes, J. Process Control 10 (April) (2000) 149–155.
[25] S.J. Qin, An overview of subspace identification, Comput. Chem. Eng. 30 (September) (2006) 1502–1513.
[26] G. Pannocchia, J.B. Rawlings, Disturbance models for offset-free model-predictive control, AICHE J. 49 (February (2)) (2003) 426–437.
[27] K.R. Muske, T.A. Badgwell, Disturbance modeling for offset-free linear model predictive control, J. Process Control 12 (August (5)) (2002) 617–632.
[28] M.V. Kothare, V. Balakrishnan, M. Morari, Robust constrained model predictive control using linear matrix inequalities, Automatica 32 (October (10)) (1996) 1361–1379.
[29] Y. Lu, Y. Arkun, Quasi-min-max MPC algorithms for LPV systems, Automatica 36 (April) (2000) 527–540.
[30] T. Zhang, G. Feng, X. Zeng, Output tracking of constrained nonlinear processes with offset-free input-to-state stable fuzzy predictive control, Automatica 45 (April) (2010) 900–909.
[31] B. Anderson, T. Brinsmead, F. Bruyne, J. Hespanha, D. Liberzon, A. Morse, Multi model adaptive control. Part 1: finite controller coverings, Int. J. Robust Nonlinear Control 10 (2000) 909–929.
[32] J.W. van Wingerden, M. Verhaegen, Subspace identification of multivariable LPV systems: the PBSID approach, in: Proc. 47th IEEE Conference on Decision and Control, December, 2008, pp. 4516–4521.
[33] F. Felici, J.W. van Wingerden, M. Verhaegen, Subspace identification of MIMO LPV systems using a periodic scheduling sequence, Automotica 43 (December (10)) (2007) 1684–1697.
[34] G. Feng, A survey on analysis and design of model-based fuzzy control systems, IEEE Trans. Fuzzy Syst. 14 (October (5)) (2006) 676–697.